



Computational study and predictive investigation of the inhibitory behavior of Geranium essential oil: DFT calculation, Monte Carlo simulation and POM analyses

WAFAA ZRIOUEL ^{a*}, AZIZ BENTIS ^b, SANAA MAJID ^c, BELKHEIR HAMMOUTI ^d, SAID GMOUH ^a

^a Laboratory of Engineering and Materials (LIMAT), Faculty of Sciences Ben M'sick, Hassan II University of Casablanca, 7955, Casablanca, Morocco

^b Multi-laboratory LC2A, N°182 Industrial zone, Mohammedia, Morocco

^c Laboratory of Materials Engineering for the Environment and Valorization (GeMEV), Faculty of Sciences Ain Chock, Hassan II University of Casablanca, 5366, Casablanca, Morocco

^d Euro-Mediterranean University of Fes, BP 51, Fes 30070, Morocco

[*wafaa.zriouel@gmail.com](mailto:wafaa.zriouel@gmail.com)

Abstract

This work presents a comprehensive computational study aimed at exploring the inhibitory potential of Geranium essential oil against corrosion. Utilizing Density Functional Theory (DFT) calculations, Monte Carlo simulations, and Petra/Osiris/Molinspiration (POM) analysis, we investigated the molecular interactions underlying the corrosion inhibition properties of Geranium oil. Our computational analyses identified key compounds within Geranium oil, characterized by high alcohol content, oxygenation, esterification, and terpene composition. These compounds exhibited diverse electron-donating and accepting capabilities, stability profiles, and reactivity patterns, highlighting their potential as effective corrosion inhibitors. The results of the Monte Carlo simulation reveal a significant variation in the adsorption of Geranium oil molecules depending on the phase. The adsorption of all the molecules studied is favored in the aqueous phase. Which means that these molecules tend to adhere to surfaces, likely a solid surface like Iron (110), more effectively when they are in an aqueous environment rather than in the gas phase. Using the Petra/Osiris/Molinspiration (POM) analysis, we calculated different properties of all molecules, namely the miLogP which indicates the molecules' lipophilicity, and can influence their affinity for hydrophobic regions on a metal surface. The topological polar surface area (TPSA) which measures the polar surface area, highlighting potential for polar interactions. The number of atoms (natoms) and the molecular weight (MW) offer insights into molecular size and complexity, impacting the ability to form protective films. The number of hydrogen bond donors (nOHNH) and the number of hydrogen bond acceptors (nOH) which relate to hydrogen bonding capabilities, and which play a role in stabilizing protective layers. Finally, the number of octet rule violations (nviolations) reflect molecular stability, while number of rotatable bonds (nrotb) indicates flexibility. In addition to the toxicity and the bioactivity score calculation.

Keywords: Corrosion inhibition, Geranium essential oil, Functional Density of Tight (DFT), Monte Carlo simulation, Petra/Osiris/Molinspiration Analysis

Introduction

Corrosion, a complex and pervasive phenomenon, has been defined by the international standard ISO 8044:2020 as "the physicochemical interaction between a metallic material and its surrounding environment, resulting in alterations to the metal's properties." This process carries substantial implications across various industries, including manufacturing and chemical plants, as well as for systems dealing with corrosive substances such as acids (Fayomi et al, 2019). In response to these challenges, and in order to avoid the often-toxic nature of conventional inhibitors used to mitigate corrosion, researchers have shifted their focus towards exploring green inhibitors sourced from plants and natural products (Oguzie et al, 2010). This research investigates the potential of Geranium essential oil, a highly valued ingredient in the perfume and cosmetic sectors (Rajesh et al, 2023), as an environmentally friendly corrosion inhibitor. The study specifically examines Rose-scented geraniums (Pelargonium species), which are cultivated in various regions such as Reunion, China, Egypt, Morocco, and India to produce "geranium oil" (Rosatoa et, 2007). The chemical composition of geranium oil varies depending on its origin. More than 240 compounds have been identified in geranium oils of diverse origins (Rosatoa et, 2007). This variation in the chemical composition explains the wide application of geranium essential oil in several fields, other than perfumery and cosmetics, such as women's health (menstrual and menopausal benefits) (Jalali-Heravi et al, 2006), skin problem and medicine as a relaxant to treat nervous tension, dysentery, hemorrhoids, inflammation, and cancer [4]. It can be used also like an insecticide (Gallardo et al, 2012), and as a food flavoring and preservation, given its antimicrobial activity (Rosatoa et, 2007- Deans et al, 1987).

The present work aims to apply a computational investigation on the all of molecules that constitute the Geranium essential oil in order to predict the mechanism of inhibition and its adsorption on the metal. To accelerate the discovery and development of this essential oil as green inhibitor for steel, we started our predictive study with the calculations of the quantum parameters by applying the density functional theory (DFT). Then, we performed the Monte Carlo simulation to confirm and complement the results found through our study. Finally, we calculated the Petra/Osiris/Molinspiration analyses to predict properties, toxicity, drug-likeness and Bioactivity of all the molecules that constitute the Geranium essential oil.

Materials and methods

Characterization of the Geranium essential oil

The Geranium essential oil was analyzed by Gas chromatography on a Clarus 580 Perkinelmer GC system coupled to a flame ionization detector (FID). The chromatographic column used was a RESTEK (60 m, 0.25 mm ID, 0.25 μm). The characteristics of the analysis are presented in the Table 1.

Injection volume	1 μl		
Injector temperature	250 C (split with split ratio of 5)		
Detector temperature (FID)	280 C		
Column	RESTEK (60 m, 0.25 mm ID, 0.25 μm)		
Detector	FID		
Carrier gas	N, H et Air 1.2, 45 et 450ml/min respectively		
Oven program	$^{\circ}\text{C}/\text{min}$	Temperature ($^{\circ}\text{C}$)	Maintain (min)
	...	50	5
	10	200	0
	5	240	2

Table 1: Operating conditions for analysis by gas chromatography GC/FID

Computational Studies of the Geranium essential oil

Quantum parameters

All calculations were performed using Materials Studio Software version 2020. Our computational investigation commenced with the optimization of the molecules under study utilizing Density Functional Theory (DFT). In order to gain insight into the molecular mechanisms governing corrosion inhibition, we computed various quantum parameters for the constituents of Geranium essential oil. These parameters included the energies of the Highest Occupied Molecular Orbital (HOMO) and the Lowest Unoccupied Molecular Orbital (LUMO), the electronic gap ($\Delta\epsilon$), as well as the absolute electronegativity (χ), absolute hardness (η), and softness (σ). These calculations were carried out in accordance with Koopmans' theorem, as mentioned in Table 2 (Chafiq et al, 2020; Xia et al, 2015 ; Pearson et al, 1998).

The quantum parameters	Calculation equation
• The highest occupied molecular orbital	$I = -\epsilon_{HOMO}$
• The lowest unoccupied molecular orbital	$A = -\epsilon_{LUMO}$
• The electronic gap	$\Delta\epsilon = \epsilon_{LUMO} - \epsilon_{HOMO}$
• The absolute electronegativity	$\chi = -\mu_i = -\left(\frac{\epsilon_{LUMO} + \epsilon_{HOMO}}{2}\right)$
• The absolute hardness	$\eta = \frac{\epsilon_{LUMO} - \epsilon_{HOMO}}{2}$
• The softness	$\sigma = \frac{1}{\eta} = \frac{2}{\epsilon_{LUMO} - \epsilon_{HOMO}}$
• The fraction of electrons transferred ΔN in the interaction of mild steel and the Geranium oil	$\Delta N = \frac{\chi_{Fe} - \chi_{inh}}{2(\eta_{Fe} + \eta_{inh})}$ <p>where $\chi_{Fe}=7$ eV mol⁻¹ and $\eta_{Fe}=0$ eV mol⁻¹ ¹ (Xia et al, 2015)</p>
• The electrophilicity index expresses the ability of an electrophile to acquire an electronic charge.	$\omega = \frac{\chi^2}{2\eta}$

Table 2: Quantum parameters to calculate with Materials Studio

Monte Carlo simulation

For each molecule comprising Geranium oil, we perform a geometric optimization using the Forcite module of Material Studio software version 2020 (BIOVIA, San Diego, CA, USA, 2020). Following that, we employ the adsorption Locator module to calculate the adsorption energy of the interaction between all of the molecules and the iron surface, specifically the Fe (110) surface, which was chosen for the simulation due to its stability (Guo et al, 2014; Obot et al, 2016), in the gas phase. For the aqueous phase, we introduce a water molecule into the simulation using the adsorption locator module.

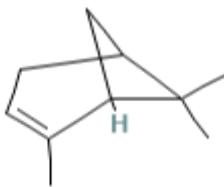
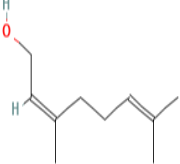
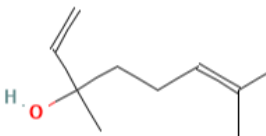
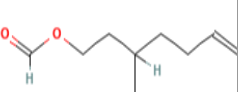
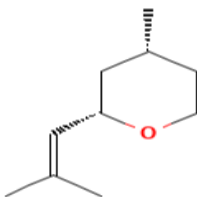
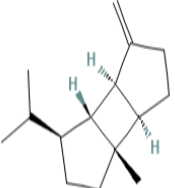
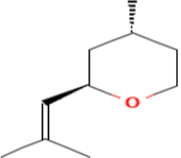
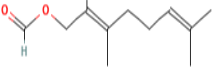
Petra/Osiris/Molinspiration (POM) Analyses

In our predictive study, we employed the POM (Petra/Osiris/Molinspiration) theory, a powerful analytical framework originally developed by Professor Taibi Ben Hadda's group in collaboration with the American NCI and TAACF. This theory was applied to assess the bioactivity score and drug-likeness of the compounds found within Geranium essential oil (Salih et al, 2023; Nadeem et al, 2016). POM, a sophisticated bioinformatics program (Chalkha et al, 2023), stands as a robust tool capable of optimizing and identifying the pharmacophore sites within organic compounds through the evaluation of physicochemical parameters. Furthermore, POM analyses provide a means to predict biological activities and facilitate the exploration of relationships between steric and electrostatic properties and biological activity.

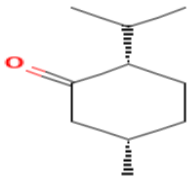
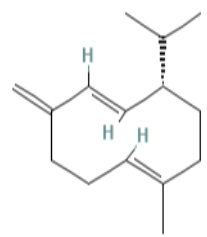

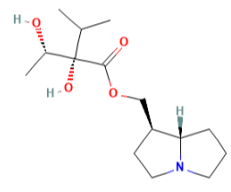
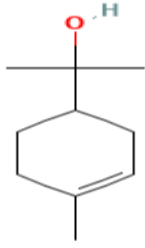
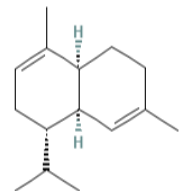
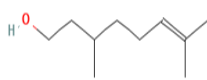
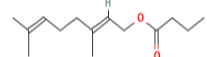
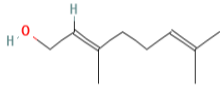
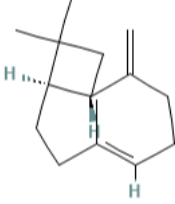
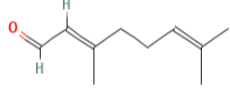
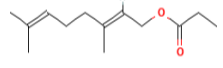
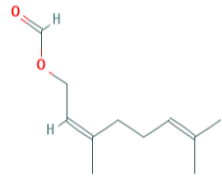
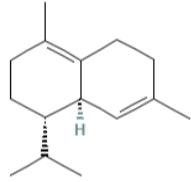
Results and discussion

The chemical composition of Geranium essential oil

The obtained constituent percentages of the Geranium essential oil, its chemical formula and its structure are summarized in Table 3.

Molecule	Structure of compound	Percentage %	Molecule	Structure of compound	Percentage %
α-pinene C₁₀H₁₆		1,75	Nerol C₁₀H₁₈O		2,10
Linalol C₁₀H₁₈O		8,55	Citronellyl formate C₁₁H₂₀O₂		9,64
Cis-rose oxide C₁₀H₁₈O		0,50	β -bourbonene C₁₅H₂₄		1,66
Trans-rose oxide C₁₀H₁₈O		3,15	Geranyl formate C₁₁H₁₈O₂		3,32

Section A-Research paper

Molecule	Structure of compound	Percentage %	Molecule	Structure of compound	Percentage %
Iso-Menthone $C_{10}H_{18}O$		8,53	Germacrene D $C_{15}H_{24}$		0,86
β-citronellol $C_{10}H_{20}O$		15,88	Viridiflore $C_{15}H_{27}NO_4$		0,62
α-Terpineol $C_{10}H_{18}O$		1,64	α-muurolene $C_{15}H_{24}$		0,30
Citronellol $C_{10}H_{20}O$		8,07	Geranyl butyrate $C_{14}H_{24}O_2$		0,24
Geraniol $C_{10}H_{18}O$		17,56	Trans-caryophyllene $C_{15}H_{24}$		0,38
(E)-citral $C_{10}H_{16}O$		1,53	Geranyl propionate $C_{13}H_{22}O_2$		0,39
Neryl formate $C_{11}H_{18}O_2$		0,29	γ-cadinene $C_{15}H_{24}$		2,87

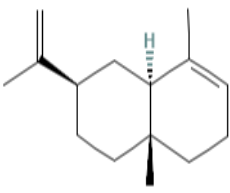
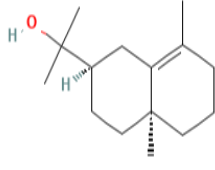
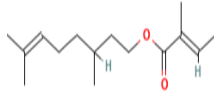
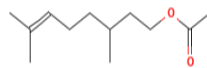
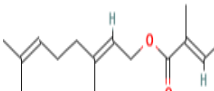
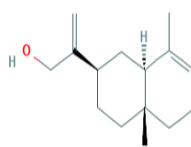
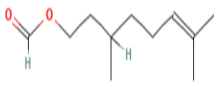
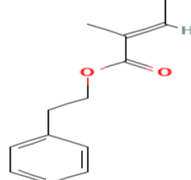
Molecule	Structure of compound	Percentage %	Molecule	Structure of compound	Percentage %
α-Selinene C₁₅H₂₄		0,51	10-epi-g-eudesmol C₁₅H₂₆O		7,29
Citronellyl tiglate C₁₅H₂₆O₂		0,41	Citronellyl acetate C₁₂H₂₂O₂		0,22
Geranyl tiglate C₁₅H₂₄O₂		0,87	α-Costol C₁₅H₂₄O		0,14
Citronellyl ester C₁₁H₂₀O₂		0,39	2-phenethyl tiglate C₁₃H₁₆O₂		0,36

Table 3: The chemical composition of Geranium essential oil obtained by GC-FID

According to the results presented in Table 3, it is evident that Geranium oil contains a significant concentration of alcohol-rich compounds, notably g eraniol (17.56%),  -citronellol (15.88%), citronellol (8.07%), and linalol (8.55%). These alcoholic compounds are known for their ability to form protective films on metallic surfaces, which can reduce reactivity with corrosive agents. Additionally, the cis and trans rose oxides (0.50% and 3.15%, respectively) as well as 10-epi-g-eudesmol (7.29%) are oxygenated compounds with antioxidant properties, which can contribute to the formation of a protective layer on the metal surface (Potapovich et al, 2011; Safitri et al, 2003).

Geranium oil also consists of esterified compounds such as neryl formate (0.29%), citronellyl formate (9.64%), geranyl formate (3.32%), and others, along with certain terpene compounds like  -cadinene (2.87%) and germacr ene D (0.86%). These terpene compounds are known for their ability to adsorb onto the metal surface.

Quantum parameters calculation

The quantum parameters of the molecules of the Geranium oil are summarized in the Table 4. The optimized geometry, LUMO and HOMO orbital of the all of molecules that constitute the Geranium oil, obtained by using the DFT in Dmol³ module of Materials Studio Software, are presented in the Table 5.

The optimization of the geometric structures of HOMO and LUMO orbitals of all of the molecules that constitute the Geranium essential oil are presented in Table 5.

Paramètre	ϵ_{HOMO}	ϵ_{LUMO}	$\Delta\epsilon$	χ (eV)	η	σ	w
	(eV)	(eV)					
α-pinene	-5.919	0.885	6.804	2.517	3.402	0.294	0.931
Linalol	-6.185	0.368	6.553	2.909	3.2765	0.305	1.291
Cis-rose oxide	-6.283	0.82	7.103	2.732	3.5515	0.282	1.050
Trans-rose oxide	-6.104	0.861	6.965	2.622	3.4825	0.287	0.987
Iso-Menthone	-6.353	-0.273	6.08	3.313	3.04	0.329	1.805
β-citronellol	-6.23	0.801	7.031	2.715	3.5155	0.284	1.048
α-Terpineol	-5.973	1.146	7.119	2.414	3.5595	0.281	0.818
Citronellol	-6.23	0.801	7.031	2.715	3.5155	0.284	1.048
Geraniol	-6.083	0.545	6.628	2.769	3.314	0.302	1.157
(E)-citral	-6.461	-1.381	5.08	3.921	2.54	0.394	3.026
Neryl formate	-6.23	0.183	6.413	3.139	3.2065	0.312	1.536
Nerol	-6.411	0.404	6.815	3.004	3.4075	0.293	1.324
Citronellyl formate	-6.258	0.183	6.441	3.038	3.2205	0.311	1.432
β-bourbonene	-6.271	0.578	6.849	2.847	3.4245	0.292	1.183
Geranyl formate	-6.249	0.142	6.391	3.054	3.1955	0.313	1.459
Germacrene D	-5.375	-0.019	5.356	2.697	2.678	0.373	1.358
Viridiflorine	-5.197	-0.504	4.693	2.851	2.347	0.426	1.731
α-muurolene	-6.012	0.851	6.863	2.581	3.4315	0.291	0.970
Geranyl butyrate	-6.034	0.4	6.434	2.817	3.217	0.311	1.233
Trans-caryophyllene	-5.915	0.59	6.505	2.663	3.2525	0.307	1.090
Geranyl propionate	-6.158	0.3	6.458	2.929	3.229	0.310	1.328
γ-cadinene	-5.804	1.004	6.808	2.4	3.404	0.294	0.846
10-epi-g-eudesmol	-5.761	0.998	6.759	2.382	3.3795	0.296	0.839
Citronellyl acetate	-6.234	0.409	6.643	2.913	3.3215	0.301	1.277
α-Costol	-6.028	0.282	6.31	2.873	3.155	0.317	1.308
2-phenethyl tiglate	-6.503	-0.684	5.819	3.594	2.9095	0.344	2.219
α-Selinene	-6.022	0.878	6.9	2.572	3.45	0.290	0.959
Citronellyl tiglate	-6.175	0.688	6.863	2.744	3.4315	0.291	1.097
Geranyl tiglate	-6.112	-0.642	5.47	3.377	2.735	0.366	2.085

Table 4: The Quantum parameters of all of the molecules comprising in the Geranium essential oil obtained by Dmol3/DFT

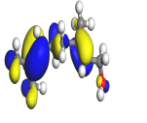
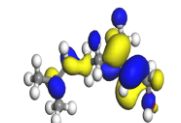
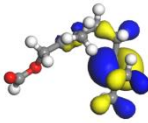
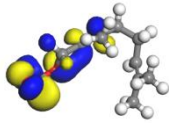
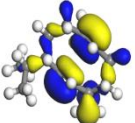
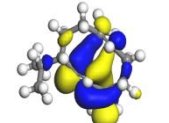
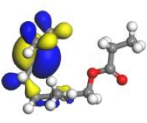
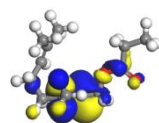
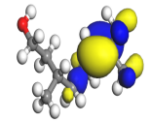
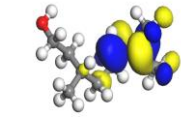
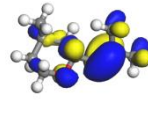
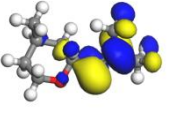
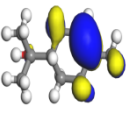
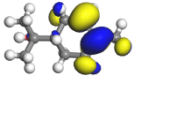
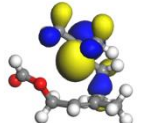
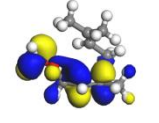
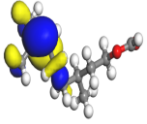
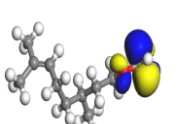
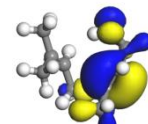
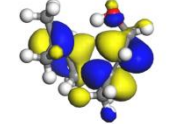
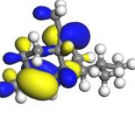

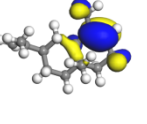
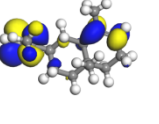
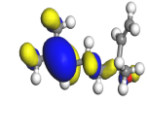
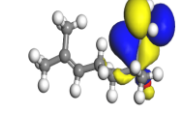
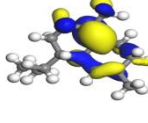
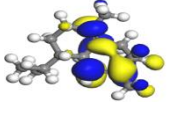
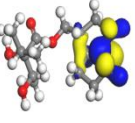
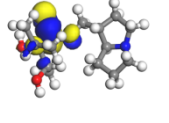
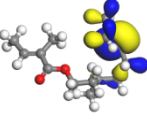
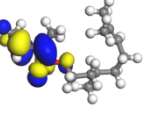
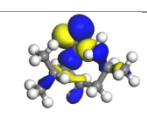
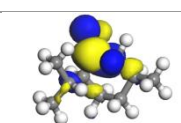
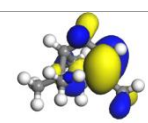
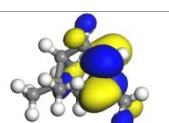
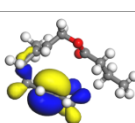
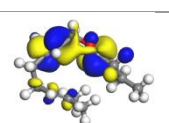
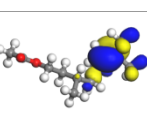
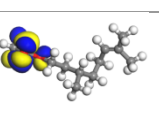
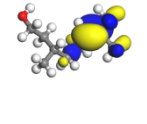
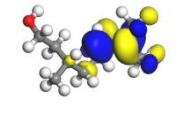
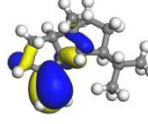
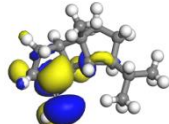
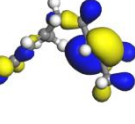
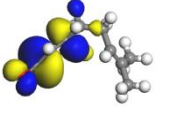
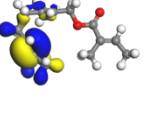
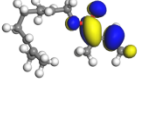
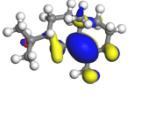
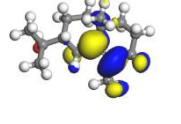
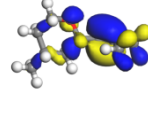
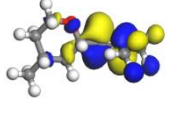
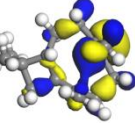
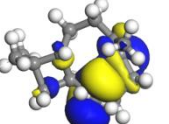
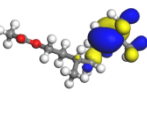
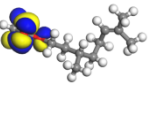
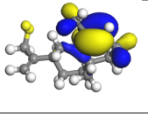
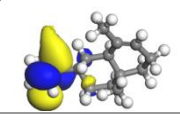
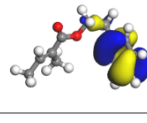
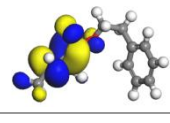
Molecule	HOMO	LUMO	Molecule	HOMO	LUMO	Molecule	HOMO	LUMO	Molecule	HOMO	LUMO
Geraniol			Geranyl formate			Germacrene D			Geranyl propionate		
β -citronellol			Trans-rose oxide			α -Terpineol			Neryl formate		
Citronellyl formate			Nerol			α -muurolene			α -Selinene		
Linalool			γ -cadinene			Viridiflore			Citronellyl tiglate		
Iso-Menthone			α -pinene			Geranyl butyrate			Citronellyl acetate		
Citronellol			β -bourbonene			(E)-citral			Geranyl tiglate		
10-epi-gudesmol			Cis-rose oxide			Trans-caryophyllene			Citronellyl ester		
α -Costol			2-phenethyl tiglate								

Table 5: The optimization of the geometric structures of HOMO and LUMO orbitals of all of the molecules that constitute the Geranium essential oil

After examining the results of the calculated quantum parameters, which are listed in Table 4, it can be observed that the molecule Viridiflorine exhibits the lowest absolute value of the HOMO orbital energy. This characteristic suggests that it has the potential to act as a potential electron donor in corrosion reactions. On the other hand, E-citral, which has the highest absolute value of the LUMO orbital energy, demonstrates a strong capacity to accept electrons. Concerning stability, alpha-Terpineol stands out as the most stable molecule, primarily due to its highest energy gap. It is followed by Citronellol and Beta-Citronellol in terms of stability. Viridiflorine is the most reactive molecule, followed by E-citral, Germacrène D, and 2-phenethyl tiglate in terms of reactivity.

Neryl formate, Nerol, Citronellyl formate, β -bourbonene, Geranyl formate, Germacrene D, Viridiflorine, α -muurolene, Geranyl butyrate, Trans-caryophyllene, Geranyl propionate, γ -cadinene, 10-epi-g-eudesmol, Citronellyl acetate, α -Costol, 2-phenethyl tiglate, α -Selinene, Citronellyl tiglate, Geranyl tiglate: These molecules exhibit various electron-donating and accepting capacities, reactivities, and variable stability levels. Their potential as corrosion inhibitors depends on their ability to interact with metal surfaces, form protective layers, and hinder corrosion processes. It is also noteworthy that the quantum parameters obtained for all molecules present similar and close values. This similarity arises from the fact that the molecules composing Geranium oil belong to chemically similar families.

Monte Carlo simulation

The energies obtained through Monte Carlo simulation, both in the aqueous and gas phases, are displayed in Table 6. In this context, the 'adsorption energy' refers to the energy released or required when the adsorbate components, in both their relaxed and unrelaxed states, are adsorbed onto the substrate. Additionally, the 'differential energy' (dE_{ad}/dEN_i) signifies the minimum energy release observed during the desorption process of a molecule from the substrate's surface. Rigid Adsorption Energy refers to the energy change when the adsorbate components are adsorbed onto the substrate without any relaxation or deformation. It represents the energy change associated with a rigid, non-flexible adsorption process.

The optimal configurations of simulations for the various molecules are presented in Table 7.

Molecule	Phases	Total energy Kcal/mol	Adsorption energy kJ/mole	Rigid adsorption energy kJ/mol	Deformation energy kJ/mol	dEad/dE Ni
Iron (110) + alpha-pinene	Gas phase	-79.477	-79.224	-80.116	0.892	-79.224
	Aqueous phase	-4638.905	-4638.905	-4937.800	298.894	-69.115
Iron (110) + Linalool	Gas phase	-130.946	-91.577	-97.710	6.133	-91.577
	Aqueous phase	-4764.988	-4764.988	-5038.292	273.303	-127.632
Iron (110) + α -Terpineol	Gas phase	-132.761	-87.158	-91.030	3.871	-87.158
	Aqueous phase	-4227.559	-4227.559	-4501.095	273.535	-108.562
Iron (110) + Germacrene D	Gas phase	-111.955	-104.494	-106.483	1.989	-104.494
	Aqueous phase	-3998.261	-3998.261	-4338.014	339.752	-90.463
Iron (110) + Cis-rose oxide	Gas phase	-125.697	-92.720	-98.607	5.886	-92.720
	Aqueous phase	-337.227	-337.27	-404.494	67.267	0.239
Iron (110) + Trans-rose oxide	Gas phase	-118.812	-87.164	-91.264	4.099	-87.164
	Aqueous phase	-3489.582	-3489.582	-3778.204	288.621	-24.034
Iron (110) + Iso-Menthone	Gas phase	-96.870	-83.954	-84.875	0.920	-83.954
	Aqueous phase	-3322.344	-3322.344	-3571.947	249.602	-46.023
Iron (110) + Beta-Citronellol	Gas phase	-114.542	-91.136	-95.024	3.887	-91.136
	Aqueous phase	-3323.379	-3323.379	-3717.755	394.376	-62.498
Iron (110) + Citronellol	Gas phase	-113.182	-89.775	-91.045	1.269	-89.775
	Aqueous phase	-3695.501	-3695.501	-3945.843	250.341	-60.126
Iron (110) + Geraniol	Gas phase	-111.445	-92.446	-96.378	3.932	-92.446
	Aqueous phase	-3746.951	-3746.953	-4018.790	271.837	-70.828
Iron (110) + E-Citral	Gas phase	-149.885	-86.457	-90.692	4.234	-86.4579
	Aqueous phase	-4120.914	-4120.916	-4397.395	276.479	-89.409
Iron (110) + Neryl Formate	Gas phase	-118.223	-99.769	-106.011	6.241	-99.769
	Aqueous phase	-4063.505	-4063.505	-4417.916	354.410	-119.308
Iron (110) + Nerol	Gas phase	-116.454	-93.396	-95.438	2.042	-93.396
	Aqueous phase	-3609.054	-3609.054	-3840.253	231.199	-88.902

Table 6 : Mulliken atomic charges for the various molecules in Geranium oil using the Dmol3/DFI module

Molecule	Phases	Total energy Kcal/mol	Adsorption energy kJ/mole	Rigid adsorption energy kJ/mol	Deformation energy kJ/mol	dEad/dE Ni
Iron (110) + Citronellyl formate	Gas phase	-127.835	-108.231	-110.928	2.697	-108.231
	Aqueous phase	-3213.830	-3213.830	-3562.169	348.338	-71.033
Iron (110) + Beta-bourbonene	Gas phase	-116.463	-103.019	-106.055	3.036	-103.019
	Aqueous phase	-2883.143	-2883.143	-3177.316	294.173	-64.426
Iron (110) + Geranyl formate	Gas phase	-132.627	-114.947	-117.721	2.774	-114.947
	Aqueous phase	-3162.985	-3162.985	-3485.409	322.423	-59.473
Iron (110) + Viridiflorine	Gas phase	-148.110	-168.049	-175.027	6.978	-168.049
	Aqueous phase	-2750.257	-2750.257	-3012.203	261.945	-54.049
Iron (110) + α -muurolene	Gas phase	-139.046	-109.676	-111.370	1.693	-109.676
	Aqueous phase	-3082.864	-3082.864	-3366.598	283.733	-63.137
Iron (110) + Geranyl butyrate	Gas phase	-157.655	-133.507	-139.983	6.475	-133.507
	Aqueous phase	-3268.122	-3268.122	-3541.974	273.852	-63.898
Iron (110) + Trans-caryophyllene	Gas phase	-121.589	-109.409	-111.754	2.344	-109.409
	Aqueous phase	-2938.206	-2938.206	-3219.879	281.673	-68.121
Iron (110) + Geranyl propionate	Gas phase	-137.581	-120.806	-123.342	2.536	-120.806
	Aqueous phase	-3168.737	-3168.737	-3417.985	249.247	-86.707
Iron (110) + Delta-Cardinene	Gas phase	-132.243	-107.080	-109.841	2.760	-107.080
	Aqueous phase	-2772.333	-2772.333	-3024.590	252.257	-53.085
Iron (110) + 10-epi-g-eudesmol	Gas phase	-164.837	-116.270	-118.558	2.288	-116.270
	Aqueous phase	-3278.423	-3278.423	-3516.875	238.452	-71.105
Iron (110) + Citronellyl acetate	Gas phase	-152.225	-116.789	-121.619	4.829	-116.789
	Aqueous phase	-2867.846	-2867.846	-3156.170	288.324	-63.624
Iron (110) + α -Costol	Gas phase	-139.222	-121.099	-125.177	4.078	-121.099
	Aqueous phase	-3269.685	-3269.685	-3695.077	425.391	-83.799
Iron (110) + 2-phenethyl tiglate	Gas phase	-142.935	-119.471	-121.960	2.489	-119.471
	Aqueous phase	-3562.149	-3562.149	-3832.524	270.374	-69.430
Iron (110) + alpha-Selinene	Gas phase	-141.413	-108.237	-111.442	3.204	-108.237
	Aqueous phase	-3086.285	-3086.285	-3337.419	251.133	-85.057

Molecule	Phases	Total energy Kcal/mol	Adsorption energy kJ/mole	Rigid adsorption energy kJ/mol	Deformation energy kJ/mol	dEad/dE Ni
Iron (110) + Citronellyl tiglate	Gas phase	-183.622	-139.092	-145.530	6.437	-139.092
	Aqueous phase	-3070.615	-3070.615	-3298.513	227.897	-69.292
Iron (110) + Geranyl tiglate	Gas phase	-176.757	-136.456	-141.513	5.056	-136.456
	Aqueous phase	-3131.545	-3131.545	-3447.440	315.895	-73.549
Iron (110) + Citronellyl ester	Gas phase	-144.762	-109.326	-112.951	3.624	-109.326
	Aqueous phase	-3059.700	-3059.700	-3319.748	260.048	-55.372

Table 6: The results of the Monte Carlo simulation of the molecules constituting Geranium oil in gas and aqueous phases

The results of the Monte Carlo simulation reveal a significant variation in the adsorption of Geranium oil molecules depending on the phase. Alpha-pinene exhibited the lowest total energy at -79.477 Kcal/mol, indicating strong adsorption. However, when considering the rigid adsorption energy and deformation energy, it's apparent that alpha-pinene's strong adsorption is due to deformation energy contributions, as its rigid adsorption energy is less favorable. Conversely, linalool had a lower total energy but a more balanced contribution from both rigid adsorption and deformation energies.

In the gas phase, cis-rose oxide exhibits relatively strong adsorption with an adsorption energy of -92.720 kJ/mol. In the aqueous phase, adsorption decreases but remains significant at -337.270 kJ/mol. The low energetic deformation in the aqueous phase indicates relatively rigid adsorption. This variation suggests that the presence of water has a significant impact on adsorption, likely due to competitive interactions between molecules and water molecules for binding sites. Geraniol shows adsorption similar to cis-rose oxide, with strong adsorption in the gas phase (-92.446 kJ/mol) and notable adsorption in the aqueous phase (-3746.953 kJ/mol). The energetic deformation in the aqueous phase is higher than that for cis-rose oxide, suggesting some molecular flexibility during adsorption in the aqueous phase.

For E-Citral, in the gas phase, the adsorption energy is -86.457 kJ/mol, while in the aqueous phase, its absolute value increases to -4120.914 kJ/mol. This significant increase suggests a strong affinity of E-Citral for the iron surface in the presence of water. Similarly, for Neryl Formate, the adsorption energy also increases from the gas phase (-99.769 kJ/mol) to the aqueous phase (-4063.505 kJ/mol), indicating improved adsorption in the presence of water. The trend continues with Nerol, showing a preference for the aqueous phase with an adsorption energy of -3609.054 kJ/mol compared to -93.396 kJ/mol in the gas phase. Citronellyl formate

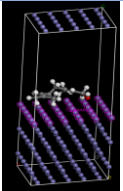
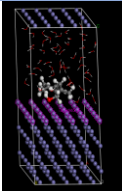
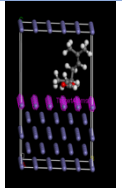
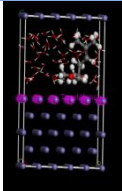
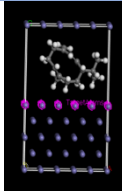
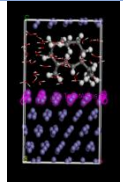
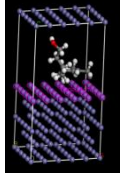
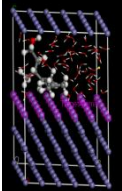
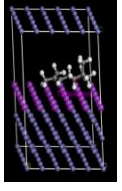
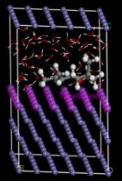
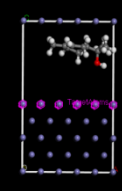
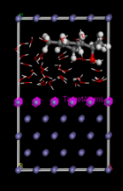
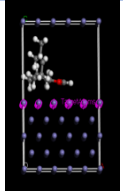
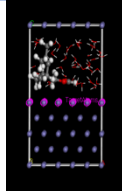
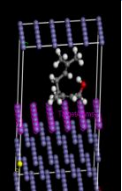
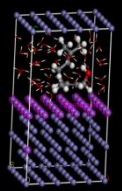
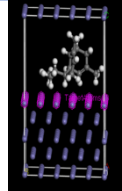
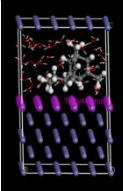
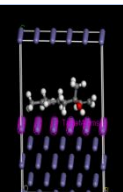
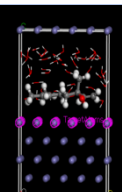
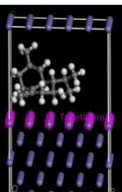
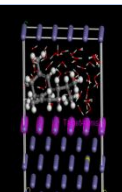
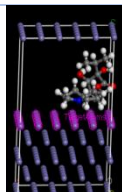
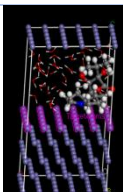
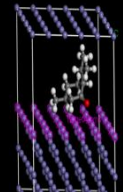
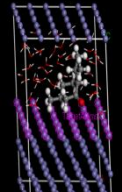
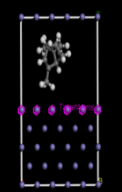
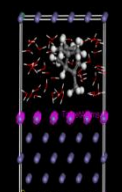
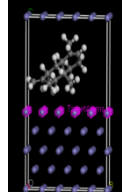
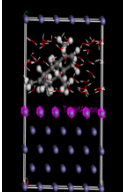
follows the same trend with better adsorption in the aqueous phase (-3213.830 kJ/mol) compared to the gas phase (-108,231 kJ/mol). For Beta-bourbonene, although adsorption is more favorable in the aqueous phase (-2883.143 kJ/mol), the difference is less pronounced compared to some other molecules. Geranyl formate exhibits a marked preference for the aqueous phase with an adsorption energy of -3162.985 kJ/mol compared to -114,947 kJ/mol in the gas phase. Viridiflorine is characterized by a preference for the aqueous phase, with an adsorption energy of -2750.257 kJ/mol, which is much higher than -168,049 kJ/mol in the gas phase. Alpha-muurolene shows a slight preference for the aqueous phase (-3082.864 kJ/mol) compared to the gas phase (-109.676 kJ/mol). Meanwhile, alpha-Costol exhibits a strong preference for the aqueous phase (-3269.685 kJ/mol) with a considerable difference in adsorption energy.

Alpha-Selinene displays significant adsorption in the gas phase (-108,237 kJ/mol), but still notable adsorption in the aqueous phase (-3086.285 kJ/mol). The energetic deformation is higher in the aqueous phase, suggesting some molecular flexibility during adsorption. In the gas phase, alpha-selinene may have a relatively rigid molecular structure when adsorbing onto the iron surface. However, in the presence of water in the aqueous phase, this molecule could undergo more significant deformation. This increased molecular flexibility in the aqueous phase may be due to specific interactions between oxygen and hydrogen atoms in water with carbon and hydrogen atoms in alpha-selinene.

POM analysis

The results of the POM analysis, obtained using two chemoinformatics software programs, namely Osiris and Molinspiration, are presented in Tables 8 and 9. In Table 8, we have summarized the properties of the studied molecules, calculated using Molinspiration. These properties include miLogP, topological polar surface area (TPSA), number of atoms (natoms), molecular weight (MW), number of hydrogen bond donors (nOHNH), number of hydrogen bond acceptors (nOH), number of octet rule violations (nviolations), number of rotatable bonds (nrotb), as well as volume. Additionally, we have included the calculation of the bioactivity score for each molecule in this table.

As for Table 9, it presents the results of the analysis of toxicity risks, drug-likeness, and Drug-Score for all the molecules, obtained using the Osiris methodology.

Molecule	Gas phase configuration	Aqueous phase configuration	Molecule	Gas phase configuration	Aqueous phase configuration	Molecule	Gas phase configuration	Aqueous phase configuration
Geraniol			Geranyl formate			Germacrene D		
β -citronellol			Trans-rose oxide			α -Terpineol		
Citronellyl formate			Nerol			α -muurolene		
Linalool			γ -cadinene			Viridiflore		
Iso-Menthone			α -pinene			α -Selinene		

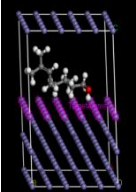
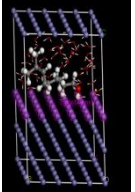
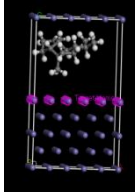
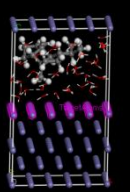
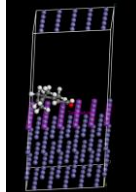
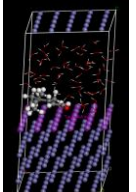
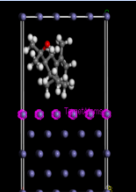
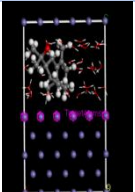
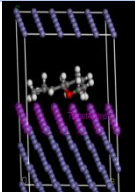
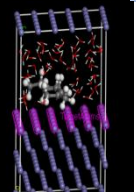
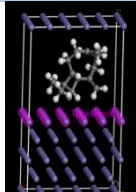
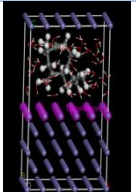
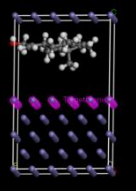
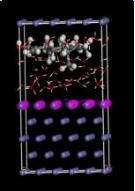
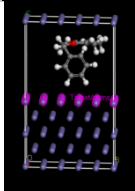
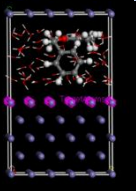
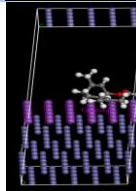
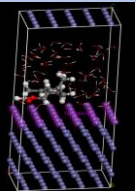
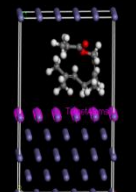
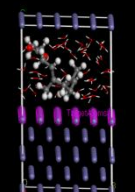
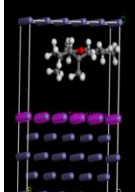
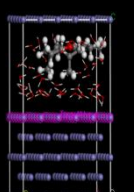
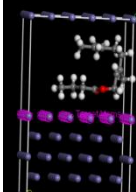
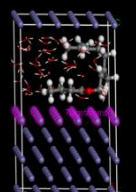
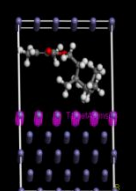
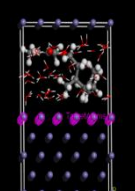
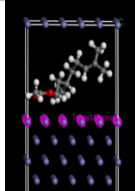
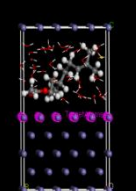
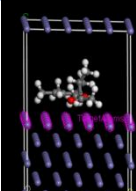
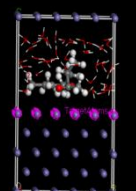
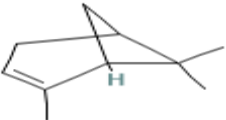
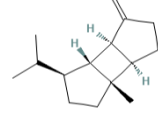
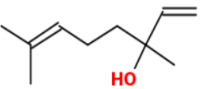
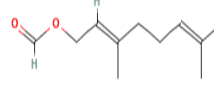
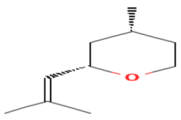
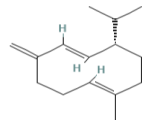
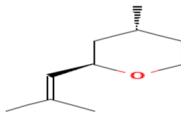
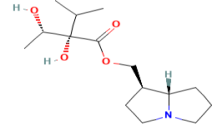
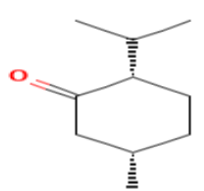
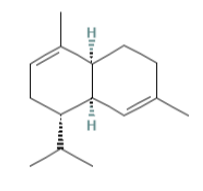
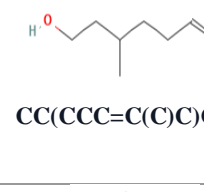
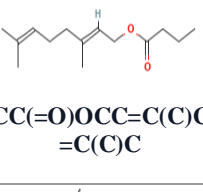
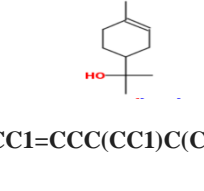
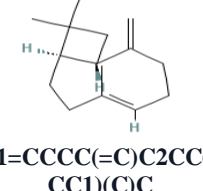
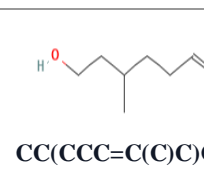
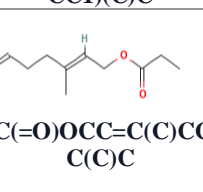
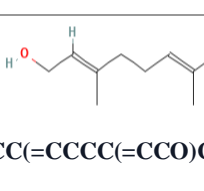
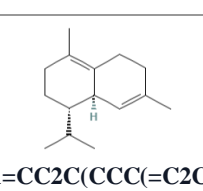
Molecule	Calculation of Molecule Property				Calculation of Bioactivity score			
Citronellol			β -bourbonene			(E)-citral		
10-epi-g-eudesmol			Cis-rose oxide			Trans-caryophyllene		
α -Costol			2-phenethyl tiglate			Neryl formate		
Geranyl propionate			Geranyl tiglate			Geranyl butyrate		
Citronellyl tiglate			Citronellyl ester			Citronellyl acetate		

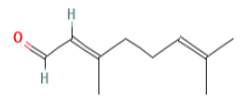
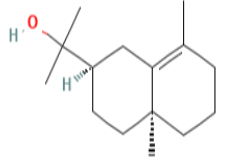
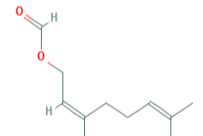
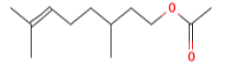
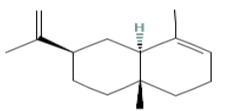
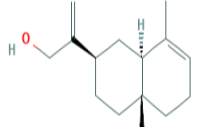
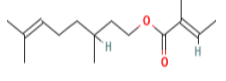
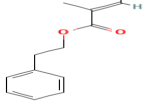
Table 7: The optimal configurations of simulations for the various molecules in gas and aqueous phases obtained by Monte Carlo

	miLogP	TPSA	natoms	MW	nON	nOHNH	nviolations	nrotb	volume	GPCR ligand	Ion channel modulator	Kinase inhibitor	Nuclear receptor ligand	Protease inhibitor	Enzyme inhibitor
α -pinene	3.54	0.00	10	136.24	0	0	0	0	151.81	-0.48	-0.43	-1.50	-0.62	-0.85	-0.34
Linalol	3.21	20.23	11	154.25	1	1	0	4	175.59	-0.73	0.07	-1.26	-0.06	-0.94	0.07
Cis-rose oxide	3.11	9.23	11	154.25	1	0	0	1	171.94	-0.77	-0.05	-1.38	-0.70	-0.87	0.03
Trans-rose oxide	3.11	9.23	11	154.25	1	0	0	1	171.94	-0.77	-0.05	-1.38	-0.70	-0.87	0.03
Iso-Menthone	3.15	17.07	11	154.25	1	0	0	1	171.35	-1.10	-0.63	-1.93	-1.10	-0.91	-0.45
β -citronellol	3.15	20.23	11	156.27	1	1	0	5	181.79	-0.81	-0.24	-1.16	-0.61	-0.83	-0.12
α -Terpineol	2.60	20.23	11	154.25	1	1	0	1	170.65	-0.51	0.15	-1.45	-0.02	-0.78	0.14
Citronellol	3.15	20.23	11	156.27	1	1	0	5	181.79	-0.81	-0.24	-1.16	-0.61	-0.83	-0.12
Geraniol	3.20	20.23	11	154.25	1	1	0	4	175.57	-0.60	0.07	-1.32	-0.20	-1.03	0.28
(E)-citral	3.65	17.07	11	152.24	1	0	0	4	169.74	-0.86	-0.25	-1.29	-0.42	-0.57	0.02
Neryl formate	3.63	26.30	13	182.26	2	0	0	6	195.53	-0.58	-0.05	-1.13	-0.28	-0.98	0.39
Nerol	3.20	20.23	11	154.25	1	1	0	4	175.57	-0.60	0.07	-1.32	-0.20	-1.03	0.28
Citronellyl formate	3.58	26.30	13	184.28	2	0	0	7	201.74	-0.62	-0.19	-0.98	-0.53	-0.67	0.18
β -bourbonene	5.54	0.00	15	204.36	0	0	1	1	225.37	-0.56	0.11	-0.95	0.13	-0.41	-0.04
Geranyl formate	3.63	26.30	13	182.26	2	0	0	6	195.53	-0.58	-0.05	-1.13	-0.28	-0.98	0.39
Germacrene D	5.43	0.00	15	204.36	0	0	1	1	234.90	-0.30	-0.11	-0.81	0.32	-0.67	0.26
Viridiflore	1.38	70.00	20	285.38	5	2	0	6	282.05	0.41	0.52	-0.24	0.22	0.33	0.11
α -muurolene	5.97	0.00	15	204.36	0	0	1	1	229.75	-0.15	0.03	-0.84	0.22	-0.74	0.28
Geranyl butyrate	4.83	26.30	16	224.34	2	0	0	8	245.69	-0.26	0.05	-0.86	0.03	-0.56	0.30
Trans-caryophyllene	5.17	0.00	15	204.36	0	0	1	0	229.95	-0.34	0.28	-0.78	0.13	-0.60	0.19
Geranyl propionate	4.27	26.30	15	210.32	2	0	0	7	228.89	-0.41	-0.12	-1.11	-0.06	-0.72	0.19
γ -cadinene	5.81	0.00	15	204.36	0	0	1	1	229.72	-0.58	-0.02	-0.75	0.00	-0.68	0.19
10-epi-g-eudesmol	4.06	20.23	16	222.37	1	1	0	1	243.28	-0.29	0.20	-0.81	0.53	-0.32	0.40
Citronellyl acetate	3.86	26.30	14	198.30	2	0	0	7	218.30	-0.54	-0.09	-0.97	-0.35	-0.50	0.01
α -Costol	4.00	20.23	16	220.36	1	1	0	2	238.21	-0.07	0.10	-0.58	0.47	-0.32	0.48
2-phenethyl tiglate	3.42	26.30	15	204.27	2	0	0	5	206.15	-0.50	-0.06	-0.93	-0.12	-0.72	0.07
α -Selinene	5.24	0.00	15	204.36	0	0	1	1	229.95	-0.24	0.12	-0.97	0.34	-0.51	0.28
Citronellyl tiglate	5.09	26.30	17	238.37	2	0	1	8	262.28	-0.36	-0.08	-0.80	0.04	-0.48	0.22
Geranyl tiglate	5.14	26.30	17	236.35	2	0	1	7	256.06	-0.33	0.03	-0.92	0.23	-0.73	0.38
Citronellyl ester	3.58	26.30	13	184.28	2	0	0	7	201.74	-0.62	-0.19	-0.98	-0.53	-0.67	0.18

Table 8: Calculation of Molecule Property and Bioactivity Score using Molinspiration Analysis

Molecule	2D structure /Canonical SMILES	Calculation of Toxicity Risks, Druglikeness and Drug-Score			Molecule	2D structure /Canonical SMILES	Calculation of Toxicity Risks, Druglikeness and Drug-Score		
α-pinene <u>C₁₀H₁₆</u>	 <chem>CC1=CCC2CC1C2(C)C</chem>	Toxicity Risks mutagenic ? tumorigenic ? irritant ? reproductive effective ?	cLogP ? 2.72	TPSA ? 0.0	Solubility ? -2.52	Druglikeness ? -1.8	Drug-Score ? 0.31	Molweight ? 136.0	
β-bourbonene <u>C₁₅H₂₄</u>	 <chem>CC(C)C1CCC2(C1C3C2CC3=C)C</chem>	Toxicity Risks mutagenic ? tumorigenic ? irritant ? reproductive effective ?	cLogP ? 4.06	TPSA ? 0.0	Solubility ? -3.79	Druglikeness ? -9.61	Drug-Score ? 0.38	Molweight ? 204.0	
Linalol <u>C₁₀H₁₈O</u>	 <chem>CC(=CCCC(C)(C=C)O)C</chem>	Toxicity Risks mutagenic ? tumorigenic ? irritant ? reproductive effective ?	cLogP ? 3.23	TPSA ? 20.23	Solubility ? -2.15	Druglikeness ? -6.68	Drug-Score ? 0.16	Molweight ? 154.0	
Geranyl formate <u>C₁₁H₁₈O₂</u>	 <chem>CC(=CCCC(=CCOC=O)C)C</chem>	Toxicity Risks mutagenic ? tumorigenic ? irritant ? reproductive effective ?	cLogP ? 3.6	TPSA ? 26.3	Solubility ? -2.47	Druglikeness ? -3.46	Drug-Score ? 0.27	Molweight ? 182.0	
Oxyde de Cis-rose <u>C₁₀H₁₈O</u>	 <chem>CC1CCOC(C1)C=C(C)C</chem>	Toxicity Risks mutagenic ? tumorigenic ? irritant ? reproductive effective ?	cLogP ? 2.74	TPSA ? 9.23	Solubility ? -2.23	Druglikeness ? -0.66	Drug-Score ? 0.37	Molweight ? 154.0	
Germacrene D <u>C₁₅H₂₄</u>	 <chem>CC1=CCCC(=C)C=CC(C)C1C(C)C</chem>	Toxicity Risks mutagenic ? tumorigenic ? irritant ? reproductive effective ?	cLogP ? 5.96	TPSA ? 0.0	Solubility ? -3.55	Druglikeness ? -10.24	Drug-Score ? 0.28	Molweight ? 204.0	
L'oxyde de Trans-rose <u>C₁₀H₁₈O</u>	 <chem>CC1CCOC(C1)C=C(C)C</chem>	Toxicity Risks mutagenic ? tumorigenic ? irritant ? reproductive effective ?	cLogP ? 2.74	TPSA ? 9.23	Solubility ? -2.23	Druglikeness ? -0.66	Drug-Score ? 0.37	Molweight ? 154.0	
Viridiflorine <u>C₁₅H₂₇NO</u>	 <chem>CC(C)C(C(C)O)(C(=O)OC1CCCN2C1CCC2)O</chem>	Toxicity Risks mutagenic ? tumorigenic ? irritant ? reproductive effective ?	cLogP ? 0.93	TPSA ? 70.0	Solubility ? -1.6	Druglikeness ? 2.02	Drug-Score ? 0.89	Molweight ? 285.0	

Molecule	2D structure /Canonical SMILES	Calculation of Toxicity Risks, Druglikeness and Drug-Score	Molecule	2D structure /Canonical SMILES	Calculation of Toxicity Risks, Druglikeness and Drug-Score
Iso-Menthone <u>C₁₀H₁₈O</u>	 <chem>CC1CCC(C(=O)C1)C(C)C</chem>	Toxicity Risks <ul style="list-style-type: none"> mutagenic <input type="checkbox"/> tumorigenic <input type="checkbox"/> irritant <input type="checkbox"/> reproductive effective <input type="checkbox"/> cLogP <input type="checkbox"/> 2.55 Solubility <input type="checkbox"/> -2.55 Molweight <input type="checkbox"/> 154.0 TPSA <input type="checkbox"/> 17.07 Druglikeness <input type="checkbox"/> -11.85 Drug-Score <input type="checkbox"/> 0.16	α-murolene <u>C₁₅H₂₄</u>	 <chem>CC1=CC2C(CC1)C(=CCC2)C(C)C</chem>	Toxicity Risks <ul style="list-style-type: none"> mutagenic <input type="checkbox"/> tumorigenic <input type="checkbox"/> irritant <input type="checkbox"/> reproductive effective <input type="checkbox"/> cLogP <input type="checkbox"/> 4.25 Solubility <input type="checkbox"/> -3.48 Molweight <input type="checkbox"/> 204.0 TPSA <input type="checkbox"/> 0.0 Druglikeness <input type="checkbox"/> -3.43 Drug-Score <input type="checkbox"/> 0.39
β-citronellol <u>C₁₀H₂₀O</u>	 <chem>CC(CCC=C(C)C)CCO</chem>	Toxicity Risks <ul style="list-style-type: none"> mutagenic <input type="checkbox"/> tumorigenic <input type="checkbox"/> irritant <input type="checkbox"/> reproductive effective <input type="checkbox"/> cLogP <input type="checkbox"/> 3.35 Solubility <input type="checkbox"/> -2.15 Molweight <input type="checkbox"/> 156.0 TPSA <input type="checkbox"/> 20.23 Druglikeness <input type="checkbox"/> -8.68 Drug-Score <input type="checkbox"/> 0.16	Geranyl butyrate <u>C₁₄H₂₄O₂</u>	 <chem>CCCC(=O)OCC=C(C)CCC=C(C)C</chem>	Toxicity Risks <ul style="list-style-type: none"> mutagenic <input type="checkbox"/> tumorigenic <input type="checkbox"/> irritant <input type="checkbox"/> reproductive effective <input type="checkbox"/> cLogP <input type="checkbox"/> 4.88 Solubility <input type="checkbox"/> -2.84 Molweight <input type="checkbox"/> 224.0 TPSA <input type="checkbox"/> 26.3 Druglikeness <input type="checkbox"/> -5.84 Drug-Score <input type="checkbox"/> 0.21
α-Terpineol	 <chem>CC1=CCC(CC1)C(C)(C)O</chem>	Toxicity Risks <ul style="list-style-type: none"> mutagenic <input type="checkbox"/> tumorigenic <input type="checkbox"/> irritant <input type="checkbox"/> reproductive effective <input type="checkbox"/> cLogP <input type="checkbox"/> 2.3 Solubility <input type="checkbox"/> -2.19 Molweight <input type="checkbox"/> 154.0 TPSA <input type="checkbox"/> 20.23 Druglikeness <input type="checkbox"/> -3.35 Drug-Score <input type="checkbox"/> 0.39	Trans-caryophyllene <u>C₁₅H₂₄</u>	 <chem>CC1=CCCC(=C)C2CC(C2)CC1(C)C</chem>	Toxicity Risks <ul style="list-style-type: none"> mutagenic <input type="checkbox"/> tumorigenic <input type="checkbox"/> irritant <input type="checkbox"/> reproductive effective <input type="checkbox"/> cLogP <input type="checkbox"/> 5.49 Solubility <input type="checkbox"/> -3.66 Molweight <input type="checkbox"/> 204.0 TPSA <input type="checkbox"/> 0.0 Druglikeness <input type="checkbox"/> -6.48 Drug-Score <input type="checkbox"/> 0.31
Citronellol <u>C₁₀H₂₀O</u>	 <chem>CC(CCC=C(C)C)CCO</chem>	Toxicity Risks <ul style="list-style-type: none"> mutagenic <input type="checkbox"/> tumorigenic <input type="checkbox"/> irritant <input type="checkbox"/> reproductive effective <input type="checkbox"/> cLogP <input type="checkbox"/> 3.35 Solubility <input type="checkbox"/> -2.15 Molweight <input type="checkbox"/> 156.0 TPSA <input type="checkbox"/> 20.23 Druglikeness <input type="checkbox"/> -8.68 Drug-Score <input type="checkbox"/> 0.16	Geranyl propionate <u>C₁₃H₂₂O₂</u>	 <chem>CCC(=O)OCC=C(C)CCC=C(C)C</chem>	Toxicity Risks <ul style="list-style-type: none"> mutagenic <input type="checkbox"/> tumorigenic <input type="checkbox"/> irritant <input type="checkbox"/> reproductive effective <input type="checkbox"/> cLogP <input type="checkbox"/> 4.42 Solubility <input type="checkbox"/> -2.57 Molweight <input type="checkbox"/> 210.0 TPSA <input type="checkbox"/> 26.3 Druglikeness <input type="checkbox"/> -1.27 Drug-Score <input type="checkbox"/> 0.28
Geraniol <u>C₁₀H₁₈O</u>	 <chem>CC(=CCCC(=CCO)C)C</chem>	Toxicity Risks <ul style="list-style-type: none"> mutagenic <input type="checkbox"/> tumorigenic <input type="checkbox"/> irritant <input type="checkbox"/> reproductive effective <input type="checkbox"/> cLogP <input type="checkbox"/> 3.49 Solubility <input type="checkbox"/> -1.89 Molweight <input type="checkbox"/> 154.0 TPSA <input type="checkbox"/> 20.23 Druglikeness <input type="checkbox"/> -3.57 Drug-Score <input type="checkbox"/> 0.45	γ-cadinene <u>C₁₅H₂₄</u>	 <chem>CC1=CC2C(CCC(=C2CC1)C)C(C)C</chem>	Toxicity Risks <ul style="list-style-type: none"> mutagenic <input type="checkbox"/> tumorigenic <input type="checkbox"/> irritant <input type="checkbox"/> reproductive effective <input type="checkbox"/> cLogP <input type="checkbox"/> 4.42 Solubility <input type="checkbox"/> -3.44 Molweight <input type="checkbox"/> 204.0 TPSA <input type="checkbox"/> 0.0 Druglikeness <input type="checkbox"/> -6.43 Drug-Score <input type="checkbox"/> 0.37

Molecule	2D structure /Canonical SMILES	Calculation of Toxicity Risks, Druglikeness and Drug-Score	Molecule	2D structure /Canonical SMILES	Calculation of Toxicity Risks, Druglikeness and Drug-Score
(E)-citral <u>C₁₀H₁₆O</u>	 CC(=CCCC(=CC=O)C)C	Toxicity Risks <ul style="list-style-type: none"> mutagenic: ? tumorigenic: ? irritant: ? reproductive effective: ? cLogP : 3.27 Solubility : -2.1 Molweight : 152.0 TPSA : 17.07 Druglikeness : -7.31 Drug-Score : 0.1	10-epi-g-eudesmol <u>C₁₅H₂₆O</u>	 CC1=C2CC(CCC2(CCC1)C)C(C)C(O)	Toxicity Risks <ul style="list-style-type: none"> mutagenic: ? tumorigenic: ? irritant: ? reproductive effective: ? cLogP : 3.73 Solubility : -3.27 Molweight : 222.0 TPSA : 20.23 Druglikeness : -4.04 Drug-Score : 0.41
Neryl formate <u>C₁₁H₁₈O₂</u>	 CC(=CCCC(=CCOC=O)C)C	Toxicity Risks <ul style="list-style-type: none"> mutagenic: ? tumorigenic: ? irritant: ? reproductive effective: ? cLogP : 3.6 Solubility : -2.47 Molweight : 182.0 TPSA : 26.3 Druglikeness : -3.46 Drug-Score : 0.27	Citronellyl acetate <u>C₁₂H₂₂O₂</u>	 CC(CCC=C(C)C)CCOC(=O)C	Toxicity Risks <ul style="list-style-type: none"> mutagenic: ? tumorigenic: ? irritant: ? reproductive effective: ? cLogP : 3.83 Solubility : -2.56 Molweight : 198.0 TPSA : 26.3 Druglikeness : -4.29 Drug-Score : 0.25
α-Selinene <u>C₁₅H₂₄</u>	 CC1=CCCC2(C1CC(CC2)C(=C)C)C	Toxicity Risks <ul style="list-style-type: none"> mutagenic: ? tumorigenic: ? irritant: ? reproductive effective: ? cLogP : 4.62 Solubility : -3.66 Molweight : 204.0 TPSA : 0.0 Druglikeness : -21.2 Drug-Score : 0.35	α-Costol <u>C₁₅H₂₄O</u>	 CC1=CCCC2(C1CC(CC2)C(=C)CO)C	Toxicity Risks <ul style="list-style-type: none"> mutagenic: ? tumorigenic: ? irritant: ? reproductive effective: ? cLogP : 3.7 Solubility : -3.15 Molweight : 220.0 TPSA : 20.23 Druglikeness : -4.68 Drug-Score : 0.33
Citronellyl tiglate <u>C₁₅H₂₆O₂</u>	 CC=C(C)C(=O)OCCC(C)C CC=C(C)C	Toxicity Risks <ul style="list-style-type: none"> mutagenic: ? tumorigenic: ? irritant: ? reproductive effective: ? cLogP : 5.1 Solubility : -3.0 Molweight : 238.0 TPSA : 26.3 Druglikeness : -5.92 Drug-Score : 0.2	2-phenethyl tiglate <u>C₁₃H₁₆O₂</u>	 CC=C(C)C(=O)OCCC1=CC=CC=C1 C=CC=C1	Toxicity Risks <ul style="list-style-type: none"> mutagenic: ? tumorigenic: ? irritant: ? reproductive effective: ? cLogP : 3.24 Solubility : -2.46 Molweight : 204.0 TPSA : 26.3 Druglikeness : -4.26 Drug-Score : 0.27

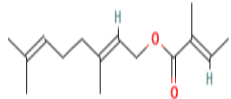


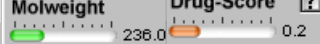
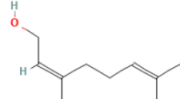
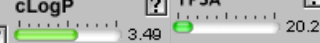

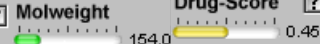
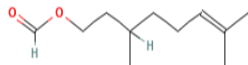

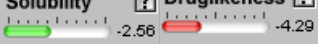
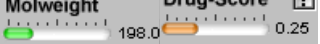


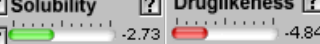

Molecule	2D structure /Canonical SMILES	Calculation of Toxicity Risks, Druglikeness and Drug-Score	Molecule	2D structure /Canonical SMILES	Calculation of Toxicity Risks, Druglikeness and Drug-Score
Geranyl tiglate <u>C₁₅H₂₄O₂</u>	 <chem>CC=C(C)C(=O)OCC=C(C)CC=C(C)C</chem>	Toxicity Risks mutagenic <input type="checkbox"/>  tumorigenic <input type="checkbox"/> Solubility <input type="checkbox"/>  irritant <input type="checkbox"/> Molweight <input type="checkbox"/>  reproductive effective <input type="checkbox"/>	Nerol	 <chem>CC(=CCCC(=CCO)C)C</chem>	Toxicity Risks mutagenic <input type="checkbox"/>  tumorigenic <input type="checkbox"/> Solubility <input type="checkbox"/>  irritant <input type="checkbox"/> Molweight <input type="checkbox"/>  reproductive effective <input type="checkbox"/>
Citronellyl ester <u>C₁₁H₂₀O₂</u>	 <chem>CC(CCC=C(C)C)CCOC(=O)C</chem>	Toxicity Risks mutagenic <input type="checkbox"/>  tumorigenic <input type="checkbox"/> Solubility <input type="checkbox"/>  irritant <input type="checkbox"/> Molweight <input type="checkbox"/>  reproductive effective <input type="checkbox"/>	Citronellyl Formate <u>C₁₁H₂₀O₂</u>	 <chem>CC(CCC=C(C)C)CCOC=O</chem>	Toxicity Risks mutagenic <input type="checkbox"/>  tumorigenic <input type="checkbox"/> Solubility <input type="checkbox"/>  irritant <input type="checkbox"/> Molweight <input type="checkbox"/>  reproductive effective <input type="checkbox"/>

Table 9: Results of Osiris calculations of all of the molecules that constitute the Geranium oil

The results of the analysis of the molecules present in geranium oil, performed using the Petra/Osiris/Molinspiration software, reveal several distinct characteristics for different components of the oil. For the alpha-pinene, this molecule stands out due to its low molecular weight and its affinity for organic phases, as evidenced by a miLogP of 3.54. However, it is important to note that its ability to interact with protein binding sites is limited, with a TPSA of 0.00. In contrast, linalool has a significantly higher TPSA of 20.23, indicating a larger potential interaction surface with proteins. Its miLogP of 3.21 suggests moderate solubility in organic phases, providing an optimal balance between hydrophobicity and hydrophilicity. Moreover, with 4 rotatable bonds, linalool offers opportunities for molecular flexibility during its interaction with biological targets.

The cis-rose oxide and trans-rose oxide isomers exhibit similar molecular properties, with a miLogP of 3.11 and a TPSA of 9.23. This suggests a moderate affinity for organic phases and a potentially favorable interaction surface for protein-molecule interactions. However, the absence of significant rotatable bonds in these molecules could influence their ability to adapt to specific binding sites.

Some compounds, such as Viridiflore, stand out due to their high TPSA values, indicating extensive surfaces conducive to interactions with proteins. They also have a high number of hydrogen and nitrogen atoms (nOHNH), suggesting a high potential for specific interactions with biological targets.

Molecules like β -bourbonene, Trans-caryophyllene, alpha-muuroolene, Delta-Cardinene, alpha-Selinene, and Germacrene D exhibit low polarity, with a TPSA close to zero, indicating less affinity for protein binding sites. Additionally, they have high miLogP values, signifying a strong affinity for organic phases. Compounds like α -Terpineol, on the other hand, display moderate affinity for proteins. It's important to note that β -bourbonene, Trans-caryophyllene, alpha-muuroolene, Delta-Cardinene, alpha-Selinene, Germacrene D, Citronellyl tiglate, and Geranyl tiglate all violate the "rule of 5," with miLogP values exceeding 5. Regarding the nuclear receptor ligand, Germacrene D, Viridiflorine, alpha-muuroolene, alpha-costol, alpha-Selinene, and Geranyl tiglate have significant values.

Finally, concerning enzymatic inhibitors, Géranol, Néryl formate, Nérol, Géranyl formate, Germacrene D, alpha-muuroolene, Géranyl butyrate, alpha-Costol, Geranyl tiglate, Citronellyl tiglate, and alpha-Selinene exhibit promising values. As for the GPCR ligand, Viridiflorine is mentioned.

The results obtained from the Osiris analysis, as mentioned in Table 9, for the 30 molecules present in geranium oil, allowed us to identify different risk categories. Firstly, it is reassuring to note that 10 out of the 30 examined molecules, namely Beta-Bourbonene, Germacrene D, Viridiflorine, alpha-muurolene, Trans-caryophyllene, Delta-Cardinene, Géraniol, 10-epi-gudesmol, alpha-Selinene, and Nérol, pose no apparent toxicity risk. These molecules can be considered safe for use in various applications.

On the other hand, a group of molecules, including alpha-pinene, Géranyl formate, linalool, cis-rose oxide, Trans-rose oxide, Iso-Menthone, Geranyl butyrate, β -citronellol, Geranyl propionate, Citronellol, Citronellyl acetate, Neryl formate, 2-phenethyl tiglate, Citronellyl tiglate, Citronellyl Formate, Citronellyl ester, and Geranyl tiglate, are considered irritants. These molecules present an irritation risk classified as red, while alpha-Costol and alpha-Terpinéol have an orange level of irritation risk.

Furthermore, only one molecule, E-Citral, has been identified as harmful in the studied geranium oil. Extreme caution is necessary when handling this molecule due to its potential harmful effects. Regarding mutagenicity risks, Linalool and Iso-menthone deserve special attention as they may pose a potential risk for genetic mutations.

Additionally, in the context of reproductive risks, Beta-Citronellol and Citronellol have been identified as potentially harmful to reproduction. These results emphasize the need for precautionary measures when using geranium oil in products or applications related to reproduction.

Conclusion

In conclusion, our predictive study of geranium essential oil as a green inhibitor for corrosion has provided valuable insights into its potential effectiveness. Through computational analyses, we have identified promising molecules within geranium oil with characteristics conducive to corrosion inhibition. These include alcohol-rich compounds, oxygenated compounds, esterified compounds, and terpenes, which exhibit various electron-donating and accepting capacities, stability levels, and reactivities.

However, to fully validate and solidify these predictions, the next step is to undertake experimental analyses. These experiments will allow us to assess the real-world corrosion inhibiting capabilities of geranium oil and its constituent molecules. This practical verification is crucial for confirming the efficacy of geranium oil as a green corrosion inhibitor.

In essence, this research serves as a crucial starting point, paving the way for further investigation and potential application of geranium essential oil in corrosion protection

strategies. Experimental validation will be instrumental in advancing the development of eco-friendly corrosion inhibition solutions and promoting sustainability in various industries.

References:

O S I Fayomi et al 2019 J. Phys.: Conf. Ser. 1378 022037

Oguzie, E. E., Enenebaku, C. K., Akalezi, C. O., Okoro, S. C., Ayuk, A. A., and Ejike, E.N. Adsorption and corrosion-inhibiting effect of *Dacryodis edulis* extract on low-carbon-steel corrosion in acidic media. *Journal of Colloid and Interface Science*. 349 (2010) 283-292

Yennam Rajesh, Nabeel M. Khan, Abdul Raziq Shaikh, Venkat S. Mane, Gaurav Daware , Ganesh Dabhade. Investigation of geranium oil extraction performance by using soxhlet extraction. *Materials Today: Proceedings* 72 (2023) 2610–2617

Essential Oils in Food Preservation, Flavor and Safety. <http://dx.doi.org/10.1016/B978-0-12-416641-7.00079-1>

Antonio Rosatoa, Cesare Vitalia, Nicolino De Laurentisa, Domenico Armenisea, Maria Antonietta Milillo. Antibacterial effect of some essential oils administered alone or in combination with Norfloxacin. *Phytomedicine* 14 (2007) 727–732

Mehdi Jalali-Heravi, Behrooz Zekavat , Hassan Sereshti . Characterization of essential oil components of Iranian geranium oil using gas chromatography–mass spectrometry combined with chemometric resolution techniques. *Journal of Chromatography A*, 1114 (2006) 154–163.

Gallardo A, Picollo MI, González-Audino P, Mougabure-Cueto G. Insecticidal activity of individual and mixed monoterpenoids of geranium essential oil against *Pediculus humanus capitis* (Phthiraptera: Pediculidae). *J Med Entomol*. 2012 Mar;49(2):332-5. doi: 10.1603/me11142. PMID: 22493851.

S.G. Deans and G. Ritchie. Antibacterial properties of plant essential oils. *International Journal of Food Microbiology*, 5 (1987) 165-180

M .Chafiq, A. Chaouiki, MR .Al-Hadeethi, R .Salghi, H .Ali Ismat, K.Mohamed Shaaban and Ill-Min Chung . A joint experimental and theoretical investigation of the corrosion inhibition behavior and mechanism of hydrazone derivatives for mild steel in HCl solution. *Colloids Surf. A*. 2020. <https://doi.org/10.1016/j.colsurfa.2020.125744>

G. Xia, X. Jiang, L. Zhou, Y. Liao, H.Wang, Q. Pu, J. Zhou . Synergic effect of methyl acrylate and N-cetylpyridinium bromide in N-cetyl-3-(2- methoxycarbonylvinyl) pyridinium bromide molecule for X70 steel protection, *Corros. Sci*, 2015, 94, 224–236.

R.G. Pearson. Absolute electronegativity and hardness: application to inorganic chemistry. *Inorg. Chem* 1998, 27, 734–740.

S Gunasekaran, S Kumaresan, R Arunbalaji, G Anand and S Srinivasan. Density functional theory study of vibrational spectra, and assignment of fundamental modes of dacarbazine. *J. Chem. Sci.*, Vol. 120, No. 3, May 2008, pp. 315–324

Materials Studio version 2020, BIOVIA, San Diego, CA, USA, 2020

L. Guo, S. Zhu, S. Zhang, Q. He and W. Li, Theoretical studies of three triazole derivatives as corrosion inhibitors for mild steel in acidic medium, *Corros. Sci.*, 2014, 87, 366–375. doi: [10.1016/j.corsci.2014.06.040](https://doi.org/10.1016/j.corsci.2014.06.040)

I.B. Obot, Savaş Kaya, Cemal Kaya, Burak Tüzün. Density Functional Theory (DFT) modeling and Monte Carlo simulation assessment of inhibition performance of some carbohydrazide Schiff bases for steel corrosion. *Physica E.* (2016), 80, 82-90. <https://doi.org/10.1016/j.physe.2016.01.024>

Salih, R. H. H.; Hasana, A. H.; Hussenc, N. H.; Hawaiz, F. E.; Hadda, T. B.; Jamalis, J.; Almalki, F. A.; Adeyinka, A. S.; Coetzee, L. C.; Oyebamiji. A. K. Thiazole-pyrazoline hybrids as potential antimicrobial agent: Synthesis, biological evaluation, molecular docking, DFT studies and POM analysis. *J. Mol. Struc.* 2023, 1282, 135191. doi: [10.1016/j.molstruc.2023.135191](https://doi.org/10.1016/j.molstruc.2023.135191)

Shafqat Nadeem, Muhammad Sirajuddin, Saeed Ahmad, Syed Ahmed Tirmizi, Muhammad Irshad Ali, Abdul Hameed. Synthesis, spectral characterization and in vitro antibacterial evaluation and Petra/Osiris/Molinspiration analyses of new Palladium(II) iodide complexes with thioamides. *Alexandria Journal of Medicine.* (2016) 52, 279-288

Chalkha, M.; El Moussaoui, A.; Hadda, T. B.; Berredjemd, M.; Bouzina, A.; Almalki, F. A.; Saghrouchnif, H.; Bakhoucha, M.; Saadi, M.; El Ammari, L.; Abdellatiifi, M. H.; El Yazidi. M. Crystallographic study, biological evaluation and DFT/POM/Docking analyses of pyrazole linked amide conjugates: Identification of antimicrobial and antitumor pharmacophore sites. *J. Mol. Struc.* 2023, 1252, 131818. doi: [10.1016/j.molstruc.2021.131818](https://doi.org/10.1016/j.molstruc.2021.131818).

Potapovich MV, Kurchenko VP, Metelitsa DI, Shadyro OI. [Antioxidant activity of oxygen-containing aromatic compounds]. *Prikl Biokhim Mikrobiol.* 2011 Jul-Aug;47(4):386-96. Russian. PMID: 21950111.

Safitri, R., Tarigan, P., Freisleben, H.J., Rumampuk, R.J. and Murakami, A. (2003), Antioxidant activity in vitro of two aromatic compounds from *Caesalpinia sappan* L. *BioFactors*, 19: 71-77. <https://doi.org/10.1002/biof.5520190109>